

Equivalent circuit model for active-layer photomixing: Parasitic-free modulation of semiconductor lasers

Kerry J. Vahala and Michael A. Newkirk

Department of Applied Physics, 128-95, California Institute of Technology, Pasadena, California 91125

(Received 27 May 1988; accepted for publication 19 July 1988)

Direct modulation of a laser diode by active-layer photomixing is studied in terms of an equivalent circuit model. The model shows that this modulation technique achieves nearly perfect immunity to package, chip, and junction-related parasitic effects so that the measured modulation response reflects the intrinsic carrier-photon dynamics. The nonlinear gain effect is included in the model.

In all commercial optical fiber communication systems employing laser diode sources, information is impressed onto the optical carrier by modulating the injection current to the laser. The maximum possible modulation rate of these devices is determined by two independent response functions. The first is the parasitic response and is caused by package and chip related impedances that tend to shunt current around the laser diode's active layer. The second is the intrinsic response determined by the interaction between the lasing mode and the optical gain medium. The latter determines a laser diode's ultimate frequency response since, in principle, package and chip-related time constants can be reduced by judicious structural design. The intrinsic response is also of fundamental importance since it gives insight into the physics of lasing action in semiconductors. In a previous letter we have demonstrated a new technique, active-layer photomixing, that permits modulation of a laser diode with nearly perfect immunity to parasitics.¹ We employed the technique to measure the intrinsic response of a transverse junction stripe laser diode and demonstrated that the response curves were indeed the theoretical ideal. In this letter we describe the physics of this measurement technique by means of an equivalent circuit model.² This enables a quantitative assessment of the technique's immunity to parasitic effects. The gain nonlinearity effect is included in the model and will be shown to have several interesting consequences of some importance to the measurement.

In active-layer photomixing the outputs from two single-frequency lasers (one tunable) are superimposed onto the active layer of a laser diode. By selecting the frequencies of the sources to fall within the band gap of the laser's cladding layers, but well above the band gap of the active layer, the two beams are selectively absorbed in the active layer. In the experiment we employed sources near a wavelength of 750 nm for photomixing in a GaAs(AlGaAs) laser diode. The absorption process results in mixing of the fields thereby generating a population of electrons and holes whose densities are modulated at the difference frequency of the sources. These carriers quickly relax to the bottom of their respective bands where they contribute to lasing action by modulating the optical gain and hence the laser diode's light output. By controlling the frequency difference of the two sources the laser diode's light output can be modulated over a wide range of frequencies. In the experiment the laser was biased to an operating point using an injection current and the single-frequency sources were used to small signal modulate the laser about this point.

The modulation created by the active-layer photomixing technique does not rely upon electronic transport processes into the device's active layer. Modulation is created where it is needed by the photomixed optical beams. Nonetheless, the modulation is loaded somewhat by device parasitic elements and it is important to determine the significance of this loading. It will be shown that such loading is, in fact, minute. The clamping of the optical gain above threshold will be seen to cause a decoupling of the intrinsic laser diode response from the external parasitic circuit as viewed by the mixed optical sources.

The laser diode, including parasitic elements, is modeled using the small-signal equivalent circuit shown in Fig. 1. The principal parasitic elements included are the bond wire inductance L , the contact resistance R , the capacitance associated with the chip itself C , and the depletion layer capacitance C_D . The impedance $Z(\omega)$ represents the small-signal impedance of the intrinsic laser diode, described in greater detail below. The current source I_M results from the carriers created by the photomixing process. These carriers are created high in their respective energy bands and relax on femto-second time scales to the bottom of the band. The relaxation process results in a small shift in the local quasi-electrochemical potentials or equivalently a charging of the depletion layer capacitance. For efficient active-layer photomixing the modulation current I_L must be large in comparison to the possible parasitic currents, I_D and I_R . Typical values for the parasitic elements are $L = 1$ nH, $R = 10$ Ω , $C = 10$ pF (1 pF for devices on semi-insulating substrates), and $C_D = 1$ –50 pF (depending upon structure and threshold

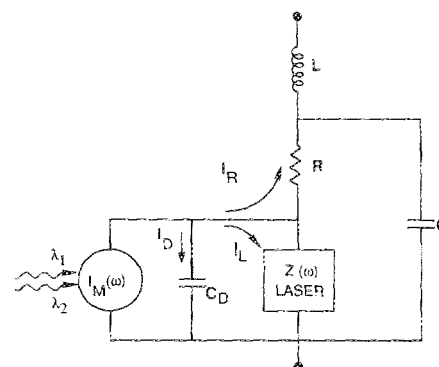


FIG. 1. Equivalent circuit model for active-layer photomixing. The photomix-induced current $I_M(\omega)$ is divided among three paths associated with the depletion layer capacitance, the intrinsic laser, and the contact resistance. The components I_D and I_R are small in comparison to I_L at all frequencies.

level excitation). The equivalent small-signal circuit model for conventional current modulation is shown in Fig. 2. For conventional current modulation the response associated with the parallel RC circuit normally determines the parasitic response function corner frequency.

The laser diode intrinsic impedance $Z(\omega)$ can be determined by solution of the rate equations in the small-signal approximation. The concept of an impedance for the intrinsic laser diode was first introduced by Harder *et al.*³ To their analysis we add the possibility of a dependence of gain on photon density (i.e., the nonlinear gain) which has recently become important in the study of laser diode dynamics.⁴ The single-mode rate equations for photon density p and carrier density n are given by

$$\dot{p} = \Gamma g(n,p)p - p/\tau + \theta, \quad (1a)$$

$$\dot{n} = -g(n,p)p - r(n) + I_L/qV, \quad (1b)$$

where Γ is the fill factor, $g(n,p)$ is the optical gain, τ is the photon lifetime, θ is the spontaneous emission rate per unit volume into the optical mode, $r(n)$ is the spontaneous recombination rate per unit volume for the carriers, I_L is the current in amperes into the intrinsic device, q is the electronic charge, and V is the active-layer volume. These equations are linearized by introducing steady-state and small-signal quantities (e.g., $n = n_0 + n_m$, where n_0 is the steady state and n_m is the time varying component) and by Taylor expanding $g(n,p)$ and $r(n)$ at the operating point. Harmonically time varying modulation is then assumed and transfer functions relating the small-signal injection current amplitude, \hat{I}_L , to the small-signal photon density amplitude, \hat{p}_m , and carrier density amplitude, \hat{n}_m , can then be found. They are given by

$$\hat{p}_m = \frac{\hat{I}_L}{qV} \frac{\Gamma g_n P_0}{\omega_R^2 - \omega^2 + i\omega\gamma}, \quad (2a)$$

$$\hat{n}_m = \frac{\hat{I}_L}{qV} \frac{i\omega + \beta}{\omega_R^2 - \omega^2 + i\omega\gamma}, \quad (2b)$$

$$\beta = \theta/P_0 - \Gamma g_p P_0, \quad (2c)$$

$$\gamma = r_n + \theta/P_0 + g_n P_0 - \Gamma g_p P_0, \quad (2d)$$

$$\omega_R^2 = g_n P_0/\tau, \quad (2e)$$

where, for example, r_n is the derivative of $r(n)$ evaluated at the operating point. The small-signal carrier density ampli-

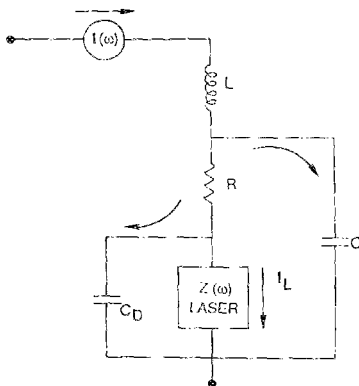


FIG. 2. Equivalent circuit model for conventional injection current modulation. The principal source of parasitic loading is shunting of the injection current $I(\omega)$ through the contact layer capacitance C .

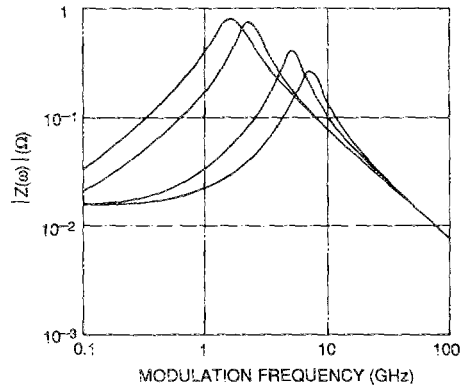


FIG. 3. Intrinsic impedance of the laser diode at output powers per facet of 0.5, 1.0, 5.0, and 10.0 mW (note: the resonant frequency increases with power). g_p is assumed finite and causes the low-frequency saturation behavior at high power.

tude can be related to the small-signal voltage across $Z(\omega)$ through the following expression³:

$$\hat{V}_m = \frac{Mk_B T}{q} \frac{\hat{n}_m}{n_0}, \quad (3a)$$

where

$$M = 2 + \frac{n_0}{2\sqrt{2}} \left(\frac{1}{N_v} + \frac{1}{N_c} \right). \quad (3b)$$

Combining (3a) and (2b) allows the intrinsic device impedance $Z(\omega)$ to be identified,

$$Z(\omega) = \frac{Mk_B T}{q^2 V n_0} \frac{i\omega + \beta}{\omega_R^2 - \omega^2 + i\omega\gamma}, \quad (4)$$

$|Z(\omega)|$ is plotted in Fig. 3 at several photon densities corresponding to laser output powers of 0.5, 1.0, 5.0, and 10.0 mW per facet in a GaAs(AIGaAs) device 250 μm in length with uncoated facets (these parameters describe the device measured in Ref. 1). The values for various parameters used in this calculation are given in Table I. The values for g_p and r_n have been determined from the experimental plot of γ vs ω_R^2 appearing in Ref. 1. From the equivalent circuit it is clear that the external parasitic loading given in terms of I_R will be insignificant provided $|Z(\omega)|$ is always small in comparison to R . (As an aside note that the reverse situation, in which a large I_R is desirable, occurs in detectors.) The maximum parasitic loading from R is, in fact, given by

$$|\hat{I}_R/\hat{I}_L|_{\max} = |Z(\omega)/R|_{\max}. \quad (5)$$

The values calculated indicate that this ratio is, indeed, very small.

The only other parasitic loading that will divert optical modulation induced current away from the laser is provided by C_D , the depletion layer capacitance. The significance of this loading is given by the following transfer function:

TABLE I. Parameter values used in calculation.

$V = 5.0 \times 10^{-11} \text{ cm}^3$	$r_n = 5.3 \times 10^9 \text{ s}^{-1}$
$g_n = 2.5 \times 10^{-6} \text{ cm}^3 \text{ s}^{-1}$	$\tau = 3 \text{ ps}$
$g_p = -6.9 \times 10^{-6} \text{ cm}^3 \text{ s}^{-1}$	$n_0 = 3 \times 10^{18} \text{ cm}^{-3}$
$\Gamma = 0.4$	$N_v = 8.2 \times 10^{18} \text{ cm}^{-3}$
$\theta = 7 \times 10^{21} \text{ cm}^{-3} \text{ s}^{-1}$	$N_c = 4.3 \times 10^{17} \text{ cm}^{-3}$

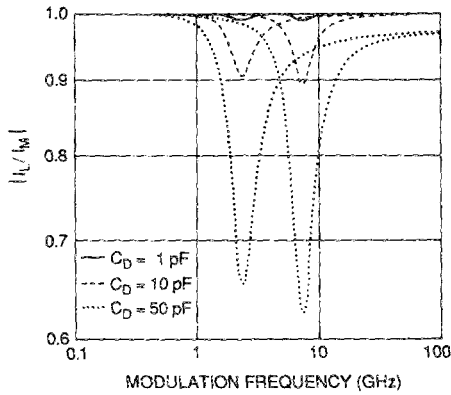


FIG. 4. Depletion-layer capacitive loading of the active-layer photomix-induced modulation for output powers per facet of 1 mW (lower frequency peaks) and 10 mW (higher-frequency peaks). Capacitance values are indicated. Loading is largest for modulation at the relaxation oscillation frequency.

$$\left| \frac{\hat{I}_L}{\hat{I}_M} \right| = \left| \frac{1}{1 + i\omega C_D Z(\omega)} \right|, \quad (6)$$

where in deriving this expression we have omitted the minute leakage through R . This transfer function has been plotted in Fig. 4 for two photon densities and at depletion capacitances of 1, 10, and 50 pF. Only for the latter case is any loading by the depletion capacitance noticeable and here only near the relaxation oscillation frequency where the intrinsic impedance experiences a temporary increase. Notice that the overall effect of this slight depletion capacitance loading is to increase the perceived damping of the relaxation resonance in the modulation response. For the structure measured in Ref. 1, however, the capacitance is estimated to be less than 10 pF so that depletion capacitance loading at the relaxation resonance is negligible.

The above analysis shows that active-layer photomixing in a semiconductor laser produces laser output modulation with nearly perfect immunity to parasitic effects at all frequencies. The analysis also shows that this is a direct consequence of $|Z(\omega)|$ being exceedingly small. The overall smallness of $|Z(\omega)|$ is caused by the tendency of the gain to be clamped at a steady-state value nearly equal to the loss rate. Gain clamping maintains the carrier density level and hence the junction voltage with changes in the injection current. The increase of $|Z(\omega)|$ near $\omega = \omega_R$ is caused by a slight unclamping of the carrier density as a result of relaxation oscillations.

It should be noted that the gain is, in fact, never perfectly clamped. The finite value of the intrinsic impedance at $\omega = 0$ reflects this fact. Most of this nonclamping in the present calculation results from the nonlinear gain effect (i.e., a nonzero g_p). Even when g_p is zero, however, the gain is not completely clamped as there is always a small difference between gain and loss made up by spontaneous emission.

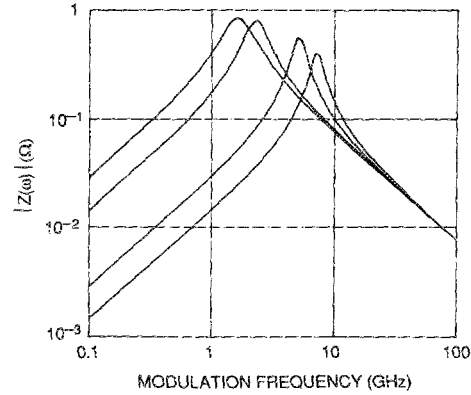


FIG. 5. Intrinsic impedance of the laser diode at output powers per facet of 0.5, 1.0, 5.0, and 10.0 mW (note: the resonant frequency increases with power). g_p is assumed to be zero. Compared to Fig. 3, this impedance function has a slightly sharper resonance and does not saturate at low frequencies.

This small difference accounts for the term involving θ in the numerator of (4). The behavior of the impedance function versus frequency and versus power is affected significantly by the nonlinear gain effect. For comparison we have plotted $|Z(\omega)|$ assuming $g_p = 0$ in Fig. 5. For g_p finite the low-frequency laser impedance saturates at high power as indicated in Fig. 3. When $g_p = 0$, however, $|Z(\omega)|$ decreases with increasing power at low frequencies (clamping is more effective), whereas the high-frequency values near the relaxation resonance are slightly larger.

In conclusion, we have presented an equivalent circuit model for modulation of a laser diode by active-layer photomixing. The model shows that this modulation technique achieves nearly perfect immunity to device parasitics and that response functions measured using the technique reflect only the intrinsic dynamics of the laser. This immunity results from the laser diode's exceedingly small intrinsic impedance which tends to decouple modulation generated by the photomixed beams from the parasitic circuit elements. We have also investigated the dependence of this impedance on the nonlinear gain effect. Its value at low frequencies saturates rather than continuing to decrease as would occur for $g_p = 0$. At frequencies near the relaxation resonance the nonlinear gain effect reduces the impedance.

This work is supported by the National Science Foundation, the Powell Foundation, and ATT Corporation.

¹M. A. Newkirk and K. J. Vahala, *Appl. Phys. Lett.* **52**, 770 (1988).

²K. J. Vahala and M. A. Newkirk, presented at the 1988 Conference on Lasers and Electro-Optics, Paper MG1.

³Ch. Harder, J. Katz, S. Margalit, J. Schacham, and A. Yariv, *IEEE J. Quantum Electron.* **QE-18**, 333 (1982).

⁴R. Olshansky, P. Hill, V. Lanzisera, and W. Powazinik, *IEEE J. Quantum Electron.* **QE-23**, 1410 (1988).